HHS Public Access

Author manuscript

Radiat Res. Author manuscript; available in PMC 2022 August 30.

Published in final edited form as:

Radiat Res. 2022 August 01; 198(2): 120–133. doi:10.1667/RADE-21-00201.1.

Female Mice are More Resistant to the Mixed-Field (67% Neutron + 33% Gamma) Radiation-Induced Injury in Bone Marrow and Small Intestine than Male Mice due to Sustained Increases in G-CSF and the Bcl-2/Bax Ratio and Lower miR-34a and MAPK Activation

Juliann G. Kiang[a,b,c,1], **Georgetta Cannon**[a], **Matthew G. Olson**[a], **Joan T. Smith**[a], **Marsha N. Anderson**[d], **Min Zhai**[a], **M. Victoria Umali**[a], **Kevin Ho**[e], **Connie Ho**[f], **Wanchang Cui**[a], **Mang Xiao**[a]

[a] Armed Forces Radiobiology Research Institute, Uniformed Services University of the Health Sciences, Bethesda, Maryland

[b] Department of Pharmacology and Molecular Therapeutics, Uniformed Services University of the Health Sciences, Bethesda, Maryland

[c] Department of Medicine, Uniformed Services University of the Health Sciences, Bethesda, Maryland

[d] NIH, Blood Bank, Bethesda, Maryland

[e] Department of Public Health, Johns Hopkins University, Baltimore, Maryland

[f] School of Medicine, University of California, Los Angeles, California

Abstract

In nuclear and radiological incidents, overexposure to ionizing radiation is life-threatening. It is evident that radiation depletes blood cells and increases circulating cytokine/chemokine concentrations as well as mortality. While microglia cells of female mice have been observed to be less damaged by radiation than in male mice, it is unclear whether sex affects physio-pathological responses in the bone marrow (BM) and gastrointestinal system (GI). We exposed B6D2F1 male and female mice to 0, 1.5, 3, or 6 Gy with mixed-field radiation containing 67% neutron and 33% gamma at a dose rate of 0.6 Gy/min. Blood and tissues were collected on days 1, 4, and 7 postirradiation. Radiation increased cytokines/chemokines in the femurs and ilea of female and male mice in a dose-dependent manner. Cytokines and chemokines reached a peak on day 4 and declined on day 7 with the exception of G-CSF which continued to increase on day 7 in female mice but not in male mice. MiR-34a (a Bcl-2 inhibitor), G-CSF (a miR-34a inhibitor), MAPK activation (pro-cell death), and citrulline (a biomarker of entroepithelial proliferation), active caspase-3 (a biomarker of apoptosis) and caspase-1 activated gasdermin D (a pyroptosis biomarker) were measured in the sternum, femur BM and ileum. Sternum histopathology analysis with H&E staining and femur BM cell counts as well as Flt-3L showed that BM cellularity was

[1] Address for correspondence: Juliann G. Kiang, 4555 South Palmer Road, Bethesda, MD 20889-5648; juliann.kiang@usuhs.edu.

not as diminished in females, with males showing a 50% greater decline on day 7 postirradiation, mainly mediated by pyroptosis as indicated by increased gasdermin D in femur BM samples. Ileum injury, such as villus height and crypt depth, was also 43% and 30%, respectively, less damaged in females than in males. The severity of injury in both sexes was consistent with the citrulline and active caspase-3 measurements as well as active caspase-1 and gasdermin D measurements, suggesting apoptosis and pyroptosis occurred. On day 7, G-CSF in the ileum of female mice continued to be elevated by sevenfold, whereas G-CSF in the ileum of male mice returned to baseline. Furthermore, G-CSF is known to inhibit miR-34a expression, which in ileum on day 1 displayed a 3- to 4-fold increase in female mice after mixed-field (67% neutron + 33% gamma) irradiation, as compared to a 5- to 9-fold increase in male mice. Moreover, miR-34a blocked Bcl-2 expression. Mixed-field (60% neutron + 33% gamma) radiation induced more Bcl-2 in females than in males. On day 7, AKT activation was found in the ileums of females and males. However, MAPK activation including ERK, JNK, and p38 showed no changes in the ileum of females (by 0-fold; $P > 0.05$), whereas the MAPK activation was increased in the ileum of males (by 100-fold; $P < 0.05$). Taken together, the results suggest that organ injury from mixed-field (67% neutron + 33% gamma) radiation is less severe in females than in males, likely due to increased G-CSF, less MAPK activation, low miR-34a and increased Bcl-2/Bax ratio.

INTRODUCTION

Threats from a radiological weapon of mass destruction are increasing. Scenarios of large-scale radiological events include the use of improvised nuclear devices (INDs) that may produce gamma rays and a significant neutron component with prompt-radiation exposure (1, 2). Studies of neutron vs. photon effects in tissues have shown differences in gene expression related to DNA damage, cell cycle delays, oxidative stress degeneration, apoptosis, and transcription (3). Double-strand breaks (DSBs) and non-DSB-clustered DNA lesions are hallmarks of high-LET radiations. Neutrons are more effective than gamma rays in inducing DNA damage as shown by decreases in DNA flexibility indicated by slower rotation of the molecules (4, 5).

Laboratory studies show that, compared with pure photon irradiation, mixed-field (neutron + gamma) irradiation causes increased mortality, decreased survival time, decreased latency in acute radiation syndrome (ARS), and delayed healing of injuries (wound and/or burn) suffered in combination with radiation (6–8). The mechanisms of injury by low-LET radiation are different from those of high-LET radiation, which may affect dose assessment and countermeasure efficacy (3, 7–9). High-LET increases C-reactive protein, complement component 3, IgM and PGE2 in circulation (10). Moreover, the reduction of blood cell counts and the increases in circulating IL-18, G-CSF and GM-CSF after high-LET irradiation (11) are greater than those observed after low-LET irradiation (12, 13). Nevertheless, there are no differences in these circulating parameters between male and female in response to high-LET and low-LET irradiation (11, 13).

We previously reported that low-LET irradiation increased IL-1β, IL-2, IL-12p40, IL-17A, G-CSF, IFN-γ, KC, MCP-1, and IL-18 expression in ileum on day 1 (14), G-CSF in spleen on day 3 and ileum, bone marrow, and kidney on day 7; KC in spleen on day 15, and KC

in ileum, bone marrow and kidney on day 7 postirradiation (12). There was no previous cytokine data available from tissues of animals exposed to mixed-field (67% neutron + 33% gamma) which we could evaluate.

While AKT (a pro-survival signal) and MAPK (an anti-survival signal) in GI were altered by low-LET irradiation (15, 16), they have not been evaluated after mixed-field (67% neutron + 33% gamma) irradiation as we have done here.

Although there are no differences in circulating parameters including G-CSF, IL-18, WBCs and FLT-3 ligand between males and females in response to high-LET and low-LET radiation (11, 13), Susanna Rosi and her colleagues (17) investigated for the first time how combined galactic cosmic radiation (GCR) exposure impacts long-term behavioral and cellular responses in male and female mice. They found that a single exposure to simulated GCR induces long-term cognitive and behavioral deficits in the male cohorts, but not in female cohorts. Their results identified sex-dependent differences in behavioral and cognitive domains. Other than the sex-induced difference in radiation sensitivity, it is evident that females survive better after surgery than males in children with high-grade glioma (18) and adults with glioblastoma (19). Kfoury et al. (20) reported that cooperative p16 and p21 action protected female astrocytes from transformation by retinoblastoma protein overexpression. Hultborn et al. (21) reported that C57/BL/6 female mice survived better than male mice after 8 Gy total-body irradiation. However, little is known about how females and males respond to mixed-field (67% neutron + 33% gamma) radiation exposure. We hypothesized that single exposure to different doses of mixed-field radiation would result in differences in organ-injury severity between females and males.

In this report, we studied radiation-sensitive organs including the bone marrow and small intestine and their possible biomolecule changes that might explain the effects of sex on differences in radiation-induced organ injury. Correlation among miR-34a (22), cytokine profiles, MAPK, and Bcl-2-Bax (16) were explored as they are known to be significantly increased after irradiation.

MATERIALS AND METHODS

Experimental Design

Tissues were harvested from B6D2F1/J mice 12–13 weeks old (obtained from the Jackson Laboratories, Bar Harbor, ME). Mice were randomly chosen for each experimental group and housed with 5 mice per cage in a facility accredited by the Association for Assessment and Accreditation of Laboratory Animal Care, International (AAALAC International). The animal room was maintained at 23°C ±3°C with 50% ± 20% relative humidity on a 12-hour light/dark cycle. Commercial rodent ration (Envigo Teklad Rodent Diet) and acidified water (pH 2.5–3.0) used to control opportunistic infections were freely available to all animals. We performed all animal handling procedures in compliance with guidelines from the National Research Council (1). Animal study was conducted according to the protocol approved by an Institutional animal care and use committee (IACUC) at Uniformed Services University of the Health Sciences (USUHS). Groups as shown on Table 1, male and female mice were randomly divided into 4 groups (N = 12) for 0 Gy, 1.5 Gy, 3 Gy and 6 Gy mixed-field

irradiation. After irradiation, tissues were collected from each radiation dose on days 1, 4, and 7 (N = 4 per group per day).

Total-Body Mixed-Field Irradiation

Total-body irradiations of mice were performed using AFRRI's 1-MW TRIGA Mark F reactor in an exposure room with thermal neutron fluences drastically diminished by gadolinium paint. The radiation fields providing various contributions to the total dose from neutrons and photons are created by varying thicknesses of water and lead shields, which have different absorption abilities with respect to radiation of these two modalities. Fields providing with 67% neutrons and 33% gamma photons of the total dose were used (23, 24). The reactor-produced energies for gammas and neutrons ranged from 10 keV to 10 MeV and from 0.1 to 10 MeV, respectively. The average gamma and neutron energy for these spectra were ~1.5 and 2 MeV, respectively. Mice were irradiated in a specially designed mouse rotator made of aerated aluminum tubes, which contained 40 mice in vertical positions. The mice were rotated at 1.5 rpm around their vertical axes during exposure while the reactor was in steady-state mode. Mice in dose cohorts (n = 4) were total-body irradiated with total doses of 1.5, 3, and 6 Gy at a dose rate of 0.6 Gy/min (reactor power approximately 110 kW). Animals were total-body irradiated or treated in the same manner but not exposed to the radiation source (sham irradiated) except that control mice were not transported to the source room. Comparison of results for sham and control groups evaluated the effects of stress induced by handling of mice as it was performed in earlier ^{60}Co gamma-ray studies (25–28). Dosimetry was performed with paired ionization chambers that had different sensitivities to neutrons and photons (29–31). A tissue-equivalent chamber filled with a tissue-equivalent gas exhibited comparable sensitivities to neutrons and photons. The paired magnesium chamber filled with argon had much higher sensitivity to photons than to neutrons. The sensitivity coefficients of each chamber in the specific radiation fields were determined by calculating spectrum-weighted averages of the gas ionization energies, stopping powers, and mass energy absorption coefficients using neutron and photon spectra of the fields.

Tissue Collection

On days 1, 4, and 7, animals were anesthetized by isoflurane then euthanized by exsanguination confirmed by cervical dislocation. Ileums, spleens, femurs, and sternums were collected and frozen at −80°C for future use.

Histological Examination of Ileums and the Bone Marrow of Sternums

On day 7, animals were anesthetized by isoflurane then euthanized by exsanguination confirmed by cervical dislocation. Ileums and sternums were collected and immediately fixed in 10% formalin. Tissue dehydration, paraffin embedding, sectioning into 5-μm-thick sections on charged glass slide, and hematoxylin and eosin (H&E) staining was then performed. Sternums were decalcified prior to paraffin sectioning. The bright field images of H&E-stained slides were acquired by Zeiss Axioscan.Z1 and analyzed using Zeiss Zen 2.5 (blue edition). Numbers of fat cells and megakaryocytes from sternum bone marrows were counted in a 40× field and the average numbers from 4 fields of each sample were reported. For ileum histopathological slides, villus height, villus depth, crypt width, and crypt circle

counts were measured and counted. The mucosal injury score was assigned to each sample according to the following observations (32): score 0: normal; score 1: void appears within the tip of villus; score 2: ruptured tip of villus without spilling inclusion; score 3: ruptured tip of villus with spilling inclusion; score 4: ruptured tip of villus with empty inclusion; and score 5: enclosed tip of villus with shortened height and decreased crypt counts. Data of 4 fields from each were averaged and reported.

Citrulline Assay

Citrulline levels in serum were quantified in duplicate using a citrulline assay kit (cat. MET-5027, Cell Biolabs) according to manufacturer's instructions. The samples were treated briefly with SDS and proteinase K to release citrulline residues. Assay reagents were then added to the samples, which reacted with citrulline to produce a chromophore. The absorbance was read at 540–560 nm.

Bone Marrow Cell Count

The skin was cut open and both femurs from the hip to the knee were collected (retaining the femur bone ends) and placed in 6-well plates (in 2 ml PBS) on ice. On the bench (for cell counts), a sterile 10 blade scalpel, sterile forceps and sterile gauze were used to scrape/pull away the muscle. The ends of the cleaned bones were carefully cut off, and the marrow flushed out of the bones with clean PBS (about 3 ml per femur) using a syringe with a 25 g needle, into 15 ml tubes (one per mouse), gently mixed to make a homogenous mixture, and centrifuged at 3,000 rpm at 4°C for 10 min. The pellets were collected, mixed with 10 ml ACK in each tube and gently pipetted up and down to re-suspend the pellet, mixed well, and incubated at 37°C for 10 min with a shake at 5min of incubation. The mixtures were centrifuged at 3,000 rpm, 4°C for 10 min. the pellets were collected and re-suspended in 10 ml PBS on ice. Bone marrow cells were counted using a Countess™ automated cell counter (Invitrogen, Carlsbad, CA). To save the pellet after counting, each sample tube was centrifuged at 3,000 rpm (i.e., 1960 rcf), 4°C for 10 min, the supernatant poured off and the cells re-suspend in residual supernatant, transferred to the appropriate microfuge tubes, and spun at 10,000 rpm, 4°C for 10 min. Supernatants were removed and the pellets were frozen at −80°C until future use (32).

Cytokine Measurements

Ileum samples on days 1, 4, and 7 (N = 4–8 per group per time point) were collected and mixed with Na^+ Hanks' solution containing 10 μl/ml protease inhibitor cocktail, 10 mM phosphatase 2 inhibitor, 10 mM phosphatase 3 inhibitor, 10 mM DTT, 5 mM EDTA and 10 mM PMSF, homogenized using Bullet Blender Homogenizer Storm (Next Advance, Averill Park, NY) for 4 min at speed 10 and centrifuged at 9,000×g for 10 min (Sorvall Legend Micro 21 Centrifuge, Thermo Electron Corp, Madison, WI). Supernatants were conserved for protein determination and stored at −80°C until use. Cytokine/chemokine concentrations were measured and analyzed using the Bio-PlexTM Cytokine Assay (Bio-Rad; Hercules, CA) following the manufacturer's directions. Briefly, serum samples and tissue lysates from each animal were diluted fourfold and examined. Data were analyzed using the LuminexH 100TM System (Luminex Corp.; Austin, TX) and quantified using MiraiBio MasterPlexH CT and QT Software (Hitachi Software Engineering America Ltd.; San Francisco, CA).

The cytokines analyzed were IL-1α IL-1β, IL-2, IL-3, IL-4, IL-5, IL-6, IL-9, IL-10, IL-12(p40), IL-12(p70), IL-13, IL-17A, eotaxin, G-CSF, GM-CSF, IFN-γ, KC, MCP-1, MIP-1α, MIP-1β, MIP-2, RANTES and TNF-α. Data were expressed as pg/mg protein in the ileum (16).

Flt-3 Ligand Measurement

Fms-like tyrosine kinase receptor 3 ligand (Flt-3L) was measured using the MSD's HT MULTI-ARRAY electro-chemiluminescence detection technology plate-format platform (Meso Scale Diagnostics, Rockville, MD) according to the manufacturer's instructions (11).

Measurements of miR-34a and −30

RNA extraction and real-time PCR were performed following the manufacturer's protocols as previously reported (33–35). Briefly, total RNA (including small RNAs) were extracted from frozen tissues using mirVana miRNA Isolation Kits (Life Technologies). Reverse transcription (RT) was performed using TaqMan® MicroRNA Reverse Transcription Kits (Applied Biosystems, Foster City, CA), and the resulting cDNAs were quantitatively amplified for miR-34a, miR-30b and U6 using TaqMan® Universal Master Mix II, with UNG and TaqMan® MicroRNA specific primers for miR-34a (ID 000426), miR-30b (ID 000602) and U6 (ID 001973) on a 7900HT Fast Real-Time PCR System (Applied Biosystems, Foster City, CA). The relative miRNA expression fold change was quantified using the 2-ΔΔCT method with U6 as the endogenous control. Mean ± S.E.M was reported for N = 4 at each condition.

Western blots

Total protein in the ileal lysates was determined with Bio-Rad reagent (Bio-Rad, Richmond, CA). Samples with 20 μg of protein in Na^+ Hanks' buffer containing 1% sodium dodecyl sulfate (SDS) and 1% 2-mercaptoethanol were resolved on SDS-polyacrylamide slab gels (Novex precast 4–20% gel, Invitrogen, Carlsbad, CA). After electrophoresis, proteins were blotted onto a polyvinylidene difluoride (PVDF) membrane (0.45 μm, Invitrogene) using a Tran-Blot Turbo System and the manufacturer's protocol (Bio-Rad, Hercules, CA). The blot was then incubated for 60 min at room temperature with 5% non-fat dried milk in tris-buffered saline-0.5% tween20 (TBST, pH = 8.6) at room temperature. After blocking, the blot was incubated with a selected antibody against cleaved caspase-1 (catalog no. 89332), active gasdermin D (catalog no. 96458) (Cell Signaling, Danvers, MA), Bax (catalog no. sc7480), Bcl-2 (catalog no. sc7382) (Santa Cruz Biotechnology, Dallas, TX), cleaved caspase-3 (catalog no. ab214430) (ABCAM, Cambridge, MA), p-AKT (catalog no. ab192623), p-ERK (catalog no. ab50011), P-JNK (catalog no. ab124956), p-p38 (catalog no. ab195049) (ABCAM, Cambridge, MA), GAPDH (catalog no. MCA-1D4) (Encor Biotech, Gainesville, FL) at an approximately final concentration of 1–2 μg/ml in TBST – 5% milk. The blot was washed 3 times (10 min each) in TBST before incubating with a 1,000X dilution of species-specific IgG peroxidase conjugate (Bio-Techne, Minneapolis, MN) in TBST for 60 min at room temperature. The blot was washed 6 times (5 min each) in TBST before detection of the peroxidase activity using the Enhanced Chemiluminescence kit (Cytiva, Marlborough, MA). IgG and GAPDH levels were not altered by radiation and were used as a control for protein loading. Protein bands of interest were quantitated using

the ImageJ program and normalized to IgG or GAPDH. Data were expressed as intensity ratio to the respective sham group (i.e., % 0 Gy) (32).

Statistical Analysis

Results were expressed as mean ± standard error of mean (SEM) unless otherwise stated. Difference among groups was analyzed by one-way or two-way ANOVA and t-test. P value less than 0.05 is considered statistically significant.

RESULTS

Mixed-Field (67% neutron + 33% gamma) Radiation Significantly Injures Bone Marrow of Male Mice more than Female Mice

Radiation decreases bone marrow cellularity, as shown by increases in fat cells and decreases in megakaryocyte counts (15). Figure 1 shows that while 1.5 Gy did not cause changes, 3 Gy mixed-field radiation significantly increased the amount of fat cells in the bone marrow of female mice and 6 Gy led to an even greater increase. The bone marrows of male mice displayed more fat cells than that of female mice (Fig. 1B). Megakaryocytes in bone marrows of male and female mice were significantly reduced by the mixed-field (67% neutron + 33% gamma) radiation in a radiation dose-dependent manner, but no difference was found between male and female mice (Fig. 1C).

For further confirmation of radiation-induced changes in bone marrow cellularity on day 7 postirradiation, bone marrow cell counts from femurs in females displayed a significant decrease at 6 Gy but not at 1.5 Gy and 3 Gy in comparison with the data at 0 Gy (Fig. 1D). The bone marrow cell counts from femurs in males displayed significant decreases at 3 Gy and 6 Gy but not at 1.5 Gy. At 6 Gy, the decreases in males were more severe than in females (Fig. 1D). The bone marrow cell counts on day 4 postirradiation were not reduced in both females and males and no differences between females and males were observed either (data not shown).

Blood concentrations of Flt-3L, a biomarker for bone marrow aplasia, were measured and found to be increased at 3 Gy and 6 Gy but not at 1.5 Gy. Their concentrations in males were significantly higher than in females (Fig. 1E), further confirming the histopathological observations. Radiation at 6 Gy reduced caspase-3 in both sexes (data not shown), but significantly increased active Gasdermin D in males (Fig. 1F), suggesting pyroptosis occurrence in males.

Mixed-field (67% Neutron + 33% Gamma) Radiation Significantly Injures Ileum of Male Mice more than Female Mice

Radiation significantly damages the gastro intestine by either shortening villus height, increasing villus width, decreasing crypt depth and counts, or increasing mucosal injury scores (15). In male mice, mixed-field (67% neutron + 33% gamma) radiation did not change the villus height at 1.5 Gy, significantly decreased the height at 3 Gy, and decreased it further at 6 Gy, while no changes were observed in female mice (Fig. 2A and B).

For the villus width as an indicator of edema, 1.5 Gy induced a significant increase in villus width compared to the sham group in male and female mice, respectively. The 3 and 6 Gy doses did not further increase the width (Fig. 2A and C).

For the crypt depth where the crypt circles reside, 1.5 Gy did not induce changes in either female or male mice. While 3 Gy significantly decreased the depth in both male and females and 6 Gy further decreased the depths in both sexes, these decreases were more significant in male mice than female mice (Fig. 2 A and D).

Mixed-field radiation significantly reduced crypt counts in a dose-response manner. However, no differences between male and female mice were found (Fig. 2E). The mucosal injury score increased with the radiation doses beginning at 1.5 Gy. A significantly greater injury score was found in male mice than in female mice (Fig. 2F).

Because significant ileum injury was observed, cleaved caspase-3 was measured. Both 1.5 Gy and 3 Gy significantly increased active caspase-3 in female and male mice, but no difference was detected between female and male mice. However, 6 Gy significantly increased active caspase-3 in male mice while it caused no increases in female mice (Fig. 2G), suggesting other types of cell death may occur (36). Figure 2H–J showed caspase-1 activation was significantly up-regulated only at 6 Gy in both genders. The males had significantly greater increases than the females. Gasdermin D was activated by caspase-1 and was increased at 3 Gy and 6 Gy in females, but at 1.5 Gy and 6 Gy in males; there were significantly more elevated levels of caspase-1 and gasdermin D in males than in females, suggesting the occurrence of pyroptosis.

Because citrulline is produced by ileum epithelium and considered to be the biomarker of the epithelial proliferation, citrulline was measured in ileum samples. Figure 3 shows that in female mice, while mixed-field radiation did not induce changes in citrulline concentration on day 1, it decreased levels on day 4 before returning to baseline on day 7. In contrast, mixed-field radiation at 3 Gy and 6 Gy significantly lowered citrulline concentrations in male mice; it stayed low on day 4 and returned to the basal level on day 7 after 3 Gy while it stayed low throughout the study after 6 Gy.

Mixed-field (67% neutron + 33% gamma) Radiation Sustains Increases in G-CSF in Ileum of Female Mice but not Males

Radiation significantly increases cytokines by elevating the expression of NF-κB/iNOS (15). Figure 4A depicts that in female mice, mixed-field radiation at 3 Gy significantly increased G-CSF on day 1 before returning to baseline on day 7, while 6 Gy significantly increased G-CSF on day 4 and sustained the increase on day 7. In male mice (Fig. 4B), 1.5 Gy and 3 Gy did not alter G-CSF levels on day 1 through day 7, whereas 6 Gy drastically increased it on day 4 before decreasing on day 7 (though it still remained significantly above the basal level). This was specific to G-CSF, because 1.5 Gy and 3 Gy did not increase KC levels on day 1 through day 7 and 6 Gy increased KC levels on day 4 which declined on day 7 in both male and female mice in a very similar fashion (Fig. 4C and D).

Other cytokine and chemokine data did not show significant differences between male and female mice after mixed-field irradiation (Supplementary Figs. S1 and S2; https://doi.org/10.1667/RADE-21-00201.1.S1).

Due to the small volume of the bone marrow samples that could be collected from irradiated mice, there was not a sufficient volume from each mouse available to perform the biochemical/molecular assays that we did with ileal samples. Therefore, the following assays were mainly conducted with ileal samples from each mouse.

Mixed-field Radiation Increases miR-34a in Ileum of Female Mice Less than Male Mice

Radiation increases miR-34a (14). As shown in Fig 5A, on day 1, in female mice, 1.5 Gy, 3 Gy, and 6 Gy significantly increased miR-34a by 3- to 4-fold ($P < 0.05$ vs. 0 Gy), whereas in male mice shown on Fig. 5B, the mixed-field irradiation significantly increased miR-34a by 5- to 9-fold ($P < 0.05$ vs. 0 Gy). On day 4, radiation increased miR-34a by 3- to 8-fold in female mice, and by 4- to 11-fold in male mice. On day 7, the increases in miR-34a were by 2- to 4-fold in female mice and by 3- to 4.5-fold in males. This disparity was specific to miR-34a, as miR-30 in male and females displayed no changes after mixed-field irradiation (Fig. 5C and D).

Mixed-field (67% Neutron + 33% Gamma) Radiation Increases Bcl-2 in Female Mice but Decreases it in Male Mice

Gamma radiation decreases Bcl-2 levels (16). In female mice, mixed-field radiation through 6 Gy did not alter Bcl-2 in the ileum on days 1 and 4 (representative gels on days 1 and 4 not shown). On day 7 (Fig. 6A), Bcl-2 levels increased after 1.5 Gy, were unaltered after 3 Gy and decreased after 6 Gy. (Fig. 6A and B). In males, 1.5 Gy and 3 Gy mixed-field radiation did not alter Bcl-2 levels on days 1 and 4 (representative gels on days 1 and 4 not shown), but decreased them on day 7 (Fig. 6A). A 6 Gy dose did not alter Bcl-2 levels on day 1, but significantly decreased them on day 4 and further decreased them on day 7 (Fig. 6A and C).

Mixed-field Radiation Differentially Decreases Bax in Female Mice and Male Mice

Gamma radiation decreases Bax (16). In female mice, mixed-field radiation at 1.5 Gy and 3 Gy did not alter Bax in the ileum on days 1 and 4 (representative gels on days 1 and 4 not shown); while 6 Gy decreased it on day 7 (Fig. 7A and B) but not 1.5 Gy and 3 Gy (Fig. 7B). In male mice, 1.5 Gy did not alter Bax on days 1, 4 (representative gels on days 1 and 4 not shown) and 7 (Fig. 7A and C); 3 Gy did not decrease it until day 7 (Fig. 7A and C); 6 Gy did not alter it on day 1, but decreased it on day 4 (Fig. 7C), and further decreased it on day 7 (Fig. 7A and C).

Mixed-field (67% Neutron + 33% Gamma) Radiation Increases Bcl-2/Bax Ratio in Female Mice and Decreases it in Male Mice

The ratio between Bcl-2 and Bax has been used as an index of cell survival. A ratio above 1 indicates an excess of Bcl-2 compared to Bax which inhibits apoptosis, whereas below 1 suggests excess Bax which drives apoptosis (15). In female mice, although the ratio is below 1 for 6 Gy on day 4, the ratios on day 7 were above 1 (Fig. 8A). In male mice, the ratios

were all below 1 (Fig. 8B), suggesting ileal cells of male mice are more likely to undergo apoptosis compared to female mice.

The Effects of Mixed-field (67% Neutron + 33% Gamma) Radiation on AKT and MAPK Activation are More Variable than those of Gamma Radiation

Gamma radiation decreases AKT activation (p-AKT) and increases MAPK activation (p-MAPK) (15). In the ileum of female and male mice on day 7, mixed-field radiation at 6 Gy but not 1.5 Gy and 3 Gy, increased p-AKT (Fig. 9A and B). However, in female mice, 1.5 Gy and 6 Gy did not alter p-ERK, p-JNK and p-MAPK; 3 Gy increased p-ERK, p-JNK and p-MAPK. In male mice, on day 7, 1.5 Gy and 6 Gy, but not 3 Gy significantly increased p-ERK, p-JNK and p-P38, suggesting different patterns in females and males responding to mixed-field irradiation.

DISCUSSION

This report is the first to investigate the effects of sex on radiation sensitivity in organs other than brains after mixed-field irradiation. The changes in bone marrow cellularity and ileum integrity were radiation dose-dependent. In both cases, female mouse tissues sustained less injury than male mouse tissues. The observations agree with data presented on brains that showed less impact in the brain of female mice than of male mice (17, 37) as well as a median survival time in females 5 days longer than in males (21).

Many studies (15, 38–40) report that radiation-injured stem cells trigger mesenchymal stem cells which enter into the fat lineage and fill in the marrow vacated void space with fat cells, suggesting the suppression of hematopoietic cell repopulation by mesenchymal stem cells and implying that mesenchymal stem cells negatively regulate hematopoietic progenitor cells. Our studies show that male mice display greater bone marrow depletion/fat cell replacement than female mice after mixed-field radiation, suggesting a reduced repair capability in male mice.

Histopathology of the GI exhibited significantly more injury in male mice than in female mice. The mucosal injury was supported, at least partially, by the data of active caspase-3 levels at 6 Gy in males. Increases in caspase-1 and gasdermin D levels were indicative of pyroptosis playing a critical role (41). The decreases in citrulline further supported the damage of epithelial cells, because citrulline is produced by enterocytes and is proportional to the number of enterocytes (42). The enterocyte reduction could be due to a reduced capability of crypts to replenish the villus enterocytes or to rapid enterocyte death, with a speed beyond the crypt's ability to replace the cells. Our data showing a great reduction of crypt depth in male mice compared to female mice supports the latter proposition. The greater increases in miR-34a found in the ilea of male mice compared to female mice further support it, because miR-34a effectively inhibits Bcl-2 (43). Activation of p53 results in increased expression of miR-34a (44) and is also implicated in directing leader cell development during wound healing (45). Whether there is a radiation response disparity to p53 activation between male and females cannot be excluded and deserves to be explored. Robin and his colleagues (20) reported that *Nf1*−/−*iDNp53* astrocytes in female mice respond with increased p16 and p21 activity and cell cycle arrest. In contrast, the *Nf1*−/

−*iDNp53* astrocytes in male mice continue to proliferate and exhibit tumorigenesis. When p16 and p21 genes were knocked out, the female mice exhibit tumorigenesis as well. This is another example to demonstrate the gene disparity between female and male mice. The possibility of p16 and p21 activity being involved in the sex-dependent radiation disparity cannot be excluded. However, it should be kept in mind that Narendran and her colleagues (46) reported women may be at significantly greater risk of suffering and dying from the radiation-induced cancer than men exposed to the same dose of radiation.

Radiation increases the expression of several cytokines (15). Among them, G-CSF is remarkably increased and has been considered mechanistically to be a self-defensive response (47). It has become a successful therapeutic treatment for acute hematopoietic syndrome (48), although it has side effects including bone pain (49), exhaustion of neutrophils in the bone marrow (50), and large-vessel vasculitis (51). Nevertheless, G-CSF was reported to effectively inhibit miR-34a (43) in addition to effectively increasing survival from lethal irradiation in female mice (52) and male mice (21). The observation of sustained increases in G-CSF in female mice and lower increases in miR-34a on day 7 after 6 Gy irradiation in comparison with those data in male mice are highly likely to contribute to the view that female mice are more resistant to mixed-field irradiation than male mice. Therefore, for medical management of organ injuries caused by irradiation, the sex-dependent disparity should be considered.

Apoptotic cell death occurs after irradiation (17). In this strain of mice, we previously reported that radiation decreased AKT activation and increased MAPK-ERK, and JNK in the cerebellum. The decrease in AKT activation was associated with p53-mdm2 regulation (53). In females, 3 Gy but not 6 Gy increased MAPK activation, whereas in males, 6 Gy but not 3 Gy increased their activation, suggesting the involvement of different pathways. Because 3 Gy is a sublethal dose, changes caused by this radiation dose were not concerning. In contrast, 6 Gy is lethal and increased MAPK activation, suggesting participating in cell death in males. Whether the MAPK activation leads to p53-mediated apoptosis is not clear and should be explored. Herein, p53 is known to increase miR-34a which is inhibited by G-CSF, thereby leading to the Bcl-2/Bax ratio being above the sham group (=1) in female mice while it is below the sham group in male mice. This reinforces the view that G-CSF plays a key role in limiting apoptotic cell death.

Figure 10 is a schematic to indicate the possible steps of cell signaling post mixed-field irradiation. Irradiation induces DNA double strand breaks (54, 55) and miR-34a (14). DNA damage-induced p53 activation may stimulate increases in miR-34a and Bax production. Cell apoptosis may be increased due to p53-induced Bax increases and miR-34a-induced Bcl-2 decreases. The sustained increases in G-CSF in female mice may inhibit miR-34a production. Subsequently, Bcl-2 production may be increased due to G-CSF-induced miR-34a inhibition (43). Therefore, apoptotic death is reduced. Furthermore, gasdermin D-mediated pyroptosis appears to play a role in disparity of radiation sensitivity between females and males as well.

In summary, mixed-field (67% neutron + 33% gamma) radiation induced more bone marrow injury and ileum damage in male mice than in female mice through the continuous G-CSF

increases, reduced miR-34a increases, increases in Bcl-2/Bax ratio, and no MAPK activation in the ileum of female mice. These results taken together suggest that female mice are more resistant to mixed-field (67% neutron + 33% gamma) radiation than male mice, and this is probably mediated by sustained increases in G-CSF and the Bcl-2/Bax ratios and lower miR-34a and MAPK activation.

Supplementary Material

Refer to Web version on PubMed Central for supplementary material.

ACKNOWLEDGMENTS

The manuscript has been cleared by the management offices of AFRRI and USUHS. The views expressed here do not necessarily represent those of the Armed Forces Radiobiology Research Institute, the Uniformed Services University of the Health Sciences, the Department of Navy, the U.S. Department of Defense and NIH. These authors thank Dr. Natalia Ossetrova for her tissue sharing, and CDT Lucas Kopp and Dr. Dennis P. McDaniel for their technical help. This study was supported by JTCG-7 DWAM52221, NIAID R33-AI080553, and AFRRI RAB310934. Authors declare no conflict of interests.

REFERENCES

1. National Research Council. Guide for the Care and Use of Laboratory Animals. 8th ed. Washington, D.C.: National Academies Press; 2011.
2. United States Department of Homeland Security. National planning scenarios created for use in national, federal, state, and local Homeland Security preparedness activities: version 21.3 Final draft. Washington, D.C.: United States Department of Homeland Security; 2006.
3. Cary LH, Ngudiankama BF, Salber RE, Ledney GD, Whitnall MH. Efficacy of radiation countermeasures depends on radiation quality. Radiat Res. 2012; 177(5):663–75. [PubMed: 22468705]
4. Tsoulou E, Kalfas CA, Sideris EG. Changes in DNA flexibility after irradiation with gamma rays and neutrons studied with the perturbed angular correlation method. Radiat Res. 2003; 159(1):33–9. [PubMed: 12492366]
5. Tsoulou E, Kalfas CA, Sideris EG. Conformational properties of DNA after exposure to gamma rays and neutrons. Radiat Res. 2005; 163(1):90–7. [PubMed: 15606312]
6. Ledney GD, Elliott TB. The AFRRI TRIGA reactor: a summary of applications in mouse studies. PHYSOR 2010: advances in reactor physics to power the nuclear renaissance, Sheraton Station Square Hotel, Pittsburgh, Pennsylvania, USA, 9–14 May 2010. La Grange Park, Ill: American Nuclear Society, Inc., 2010.
7. Ledney GD, Elliott TB, Harding RA, Jackson WE 3rd, Inal CE, Landauer MR. WR-151327 increases resistance to Klebsiella pneumoniae infection in mixed-field- and gamma-photon-irradiated mice. Int J Radiat Biol. 2000; 76(2):261–71. [PubMed: 10716647]
8. MacVittie TJ, Monroy R, Vigneulle RM, Zeman GH, Jackson WE. The relative biological effectiveness of mixed fission-neutron-gamma radiation on the hematopoietic syndrome in the canine: effect of therapy on survival. Radiat Res. 1991; 128(1 Suppl):S29–36. [PubMed: 1924744]
9. Ledney GD, Madonna GS, Elliott TB, Moore MM, Jackson WE 3rd. Therapy of infections in mice irradiated in mixed neutron/photon fields and inflicted with wound trauma: a review of current work. Radiat Res. 1991; 128(1 Suppl):S18–28. [PubMed: 1924743]
10. Kiang JG, Ledney GD. Skin injuries reduce survival and modulate corticosterone, C-reactive protein, complement component 3, IgM, and prostaglandin E 2 after whole-body reactor-produced mixed field (n + gamma-photons) irradiation. Oxid Med Cell Longev. 2013; 2013:821541. [PubMed: 24175013]
11. Ossetrova NI, Stanton P, Krasnopolsky K, Ismail M, Doreswamy A, Hieber KP. Biomarkers for Radiation Biodosimetry and Injury Assessment after Mixed-field (Neutron and Gamma) Radiation

in the Mouse Total-body Irradiation Model. Health Phys. 2018; 115(6):727–42. [PubMed: 30299338]

12. Kiang JG, Smith JT, Hegge SR, Ossetrova NI. Circulating cytokine/chemokine concentrations respond to ionizing radiation doses but not radiation dose rates: Granulocyte-colony stimulating factor and interleukin-18. Radiat Res. 2018; 189(6):634–43. [PubMed: 29652619]
13. Ossetrova NI, Stanton P, Krasnopolsky K, Ismail M, Doreswamy A, Hieber KP. Comparison of biodosimetry biomakers for radiation dose and injury assessment after mixed-field (neutron and gamma) and pure gamma radiation in the mouse total body irradiation model. Health Phys. 2018; 115(6):743–49. [PubMed: 33289997]
14. Kiang JG, Smith JT, Anderson MN, Elliott TB, Gupta P, Balakathiresan NS, et al. Hemorrhage enhances cytokine, complement component 3, and caspase-3, and regulates microRNAs associated with intestinal damage after whole-body gamma-irradiation in combined injury. PLoS One. 2017; 12(9):e0184393. [PubMed: 28934227]
15. Kiang JG, Olabisi AO. Radiation: a poly-traumatic hit leading to multi-organ injury. Cell Biosci. 2019; 9:25. [PubMed: 30911370]
16. Kiang JG, Smith JT, Cannon G, Anderson MN, Ho C, Zhai M, et al. Ghrelin, a novel therapy, corrects cytokine and NF-κB-AKT-MAPK network and mitigates intestinal injury induced by combined radiation and skin-wound trauma. Cell Biosci. 2020; 10:63. [PubMed: 32426105]
17. Krukowski K, Grue K, Frias ES, Pietrykowski J, Jones T, Nelson G, et al. Female mice are protected from space radiation-induced maladaptive responses. Brain Behav Immun. 2018; 74:106–20. [PubMed: 30107198]
18. McKinney LC, Aquilla EM, Coffin D, Wink DA, Vodovotz Y. Ionizing radiation potentiates the induction of nitric oxide synthase by IFN-gamma and/or LPS in murine macrophage cell lines: role of TNF-alpha. J Leukoc Biol. 1998; 64(4):459–66. [PubMed: 9766626]
19. Ostrom QT, Rubin JB, Lathia JD, Berens ME, Barnholtz-Sloan JS. Females have the survival advantage in glioblastoma. Neuro Oncol. 2018; 20(4):576–77. [PubMed: 29474647]
20. Kfoury N, Sun T, Yu K, Rockwell N, Tinkum KL, Qi Z, et al. Cooperative p16 and p21 action protects female astrocytes from transformation. Acta Neuropathol Commun. 2018; 6(1):12. [PubMed: 29458417]
21. Hultborn R, Albertsson P, Ottosson S, Warnhammar E, Palm A, Palm S, et al. Radiosensitivity: Gender and order of administration of G-CSF, an experimental study in mice. Radiat Res. 2019; 191(4):335–41. [PubMed: 30730283]
22. Kiang JG, Smith JT, Anderson MN, Swift JM, Christensen CL, Gupta P, et al. Hemorrhage exacerbates radiation effects on survival, leukocytopenia, thrombopenia, erythropenia, bone marrow cell depletion and hematopoiesis, and inflammation-associated microRNAs expression in kidney. PLoS One. 2015; 10(9):e0139271. [PubMed: 26422254]
23. Elliott TB, Ledney GD, Harding RA, Henderson PL, Gerstenberg HM, Rotruck JR, et al. Mixed-field neutrons and gamma photons induce different changes in ileal bacteria and correlated sepsis in mice. Int J Radiat Biol. 1995; 68(3):311–20. [PubMed: 7561391]
24. Ledney GD, Elliott TB. Combined injury: factors with potential to impact radiation dose assessments. Health Phys. 2010; 98(2):145–52. [PubMed: 20065676]
25. Ossetrova NI, Blakely WF, Nagy V, McGann C, Ney PH, Christensen CL, et al. Non-human primate total-body irradiation model with limited and full medical supportive care including filgrastim for biodosimetry and injury assessment. Radiat Prot Dosimetry. 2016; 172(1–3):174–91. [PubMed: 27473690]
26. Ossetrova NI, Condliffe DP, Ney PH, Krasnopolsky K, Hieber KP, Rahman A, et al. Early-response biomarkers for assessment of radiation exposure in a mouse total-body irradiation model. Health Phys. 2014; 106(6):772–86. [PubMed: 24776912]
27. Ossetrova NI, Ney PH, Condliffe DP, Krasnopolsky K, Hieber KP. Acute radiation syndrome severity score system in mouse total-body irradiation model. Health Phys. 2016; 111(2):134–44. [PubMed: 27356057]
28. Ossetrova NI, Sandgren DJ, Blakely WF. Protein biomarkers for enhancement of radiation dose and injury assessment in nonhuman primate total-body irradiation model. Radiat Prot Dosimetry. 2014; 159(1–4):61–76. [PubMed: 24925901]

29. International Commission on Radiation Units and Measurements. Report 26: Neutron dosimetry for biology and medicine. J ICRU. 1976; os-14(1):1–132.
30. Wootton P, Attix FH, Awschalom M, Bloch P, Eenmaa J, Horton J, et al. Protocol for neutron beam dosimetry. New York, NY: American Association of Physicists in Medicine, Task Group No. 18 Fast Neutron Beam Dosimetry Physics Radiation Therapy Committee; 1980.
31. Goodman LJ. Practical guide to ionization chamber dosimetry at the AFRRI reactor. Bethesda, MD: Defense Nuclear Agency, Armed Forces Radiobiology Research Institute; 1985–04-01. Report No. AFRRI CR85–1. Contract No.: DNA IACRO 83–847.
32. Kiang JG, Zhai M, Lin B, Smith JT, Anderson MN, Jiang S. Co-Therapy of pegylated G-CSF and ghrelin for enhancing survival after exposure to lethal radiation. Front Pharmacol. 2021; 12:628018. [PubMed: 33603673]
33. Li XH, Ha CT, Fu D, Landauer MR, Ghosh SP, Xiao M. Delta-tocotrienol suppresses radiation-induced microRNA-30 and protects mice and human CD34 + cells from radiation injury. PLoS One. 2015; 10(3):e0122258. [PubMed: 25815474]
34. Li XH, Ha CT, Fu D, Xiao M. Micro-RNA30c negatively regulates REDD1 expression in human hematopoietic and osteoblast cells after gamma-irradiation. PLoS One. 2012; 7(11):e48700. [PubMed: 23144934]
35. Li XH, Ha CT, Xiao M. MicroRNA-30 inhibits antiapoptotic factor Mcl-1 in mouse and human hematopoietic cells after radiation exposure. Apoptosis. 2016; 21(6):708–20. [PubMed: 27032651]
36. Chen Z, Wang B, Dong J, Li Y, Zhang S, Zeng X, et al. Gut Microbiota-derived l-histidine/imidazole propionate axis fights against the radiation-induced cardiopulmonary injury. Int J Mol Sci. 2021; 22(21)
37. Tzeng WY, Wu HH, Wang CY, Chen JC, Yu L, Cherng CG. Sex Differences in stress and group housing effects on the number of newly proliferated cells and neuroblasts in middle-aged dentate gyrus. Front Behav Neurosci. 2016; 10:249. [PubMed: 28119581]
38. Horowitz MC, Berry R, Holtrup B, Sebo Z, Nelson T, Fretz JA, et al. Bone marrow adipocytes. Adipocyte. 2017; 6(3):193–204. [PubMed: 28872979]
39. Naveiras O, Nardi V, Wenzel PL, Hauschka PV, Fahey F, Daley GQ. Bone-marrow adipocytes as negative regulators of the haematopoietic microenvironment. Nature. 2009; 460(7252):259–63. [PubMed: 19516257]
40. Poglio S, Galvani S, Bour S, Andre M, Prunet-Marcassus B, Penicaud L, et al. Adipose tissue sensitivity to radiation exposure. Am J Pathol. 2009; 174(1):44–53. [PubMed: 19095959]
41. Xie GH, Chen QX, Cheng BL, Fang XM. Defensins and sepsis. Biomed Res Int. 2014; 2014:180109. [PubMed: 25210703]
42. Wang L, Zhai M, Lin B, Cui W, Hull L, Li X, et al. PEG-G-CSF and L-Citrulline combination therapy for mitigating skin wound combined radiation injury in a mouse model. Radiat Res. 2021; 196(1):113–27. [PubMed: 33914884]
43. Park IH, Song YS, Joo HW, Shen GY, Seong JH, Shin NK, et al. Role of MicroRNA-34a in anti-apoptotic effects of granulocyte-colony stimulating factor in diabetic cardiomyopathy. Diabetes Metab J. 2020; 44(1):173–85. [PubMed: 31237127]
44. Tarasov V, Jung P, Verdoodt B, Lodygin D, Epanchintsev A, Menssen A, et al. Differential regulation of microRNAs by p53 revealed by massively parallel sequencing: miR-34a is a p53 target that induces apoptosis and G1-arrest. Cell Cycle. 2007; 6(13):1586–93. [PubMed: 17554199]
45. Kozyrska K, Pilia G, Vishwakarma M, Wagstaff L, Goschorska M, Cirillo S, et al. p53 directs leader cell behavior, migration, and clearance during epithelial repair. Science. 2022; 375(6581):eabl8876. [PubMed: 35143293]
46. Narendran N, Luzhna L, Kovalchuk O. Sex difference of radiation response in occupational and accidental exposure. Front Genet. 2019; 10:260. [PubMed: 31130979]
47. Kiang JG, Jiao W, Cary LH, Mog SR, Elliott TB, Pellmar TC, et al. Wound trauma increases radiation-induced mortality by activation of iNOS pathway and elevation of cytokine concentrations and bacterial infection. Radiat Res. 2010; 173(3):319–32. [PubMed: 20199217]
48. United States Federal Drug Administration [Internet]. Neupogen approval letter. 4/30/2019. [cited 9/21/2021]. Available from: FDA Approves Radiation

Medical Countermeasure: https://www.fda.gov/emergency-preparedness-and-response/about-mcmi/fda-approves-radiation-medical-countermeasure

49. Moore DC, Pellegrino AE. Pegfilgrastim-induced bone pain: A review on incidence, risk factors, and evidence-based management. Ann Pharmacother. 2017; 51(9):797–803. [PubMed: 28423916]
50. Pfeil AM, Allcott K, Pettengell R, von Minckwitz G, Schwenkglenks M, Szabo Z. Efficacy, effectiveness and safety of long-acting granulocyte colony-stimulating factors for prophylaxis of chemotherapy-induced neutropenia in patients with cancer: a systematic review. Support Care Cancer. 2015; 23(2):525–45. [PubMed: 25284721]
51. Nakamura J, Nishi TM, Yamashita S, Nakamura H, Sato K, Oda Y, et al. Pegfilgrastim-associated large-vessel vasculitis developed during adjuvant chemotherapy for breast cancer: A case report and review of the literature. J Oncol Pharm Pract. 2020; 26(7):1785–90. [PubMed: 32188319]
52. Kiang JG, Zhai M, Liao PJ, Bolduc DL, Elliott TB, Gorbunov NV. Pegylated G-CSF inhibits blood cell depletion, increases platelets, blocks splenomegaly, and improves survival after whole-body ionizing irradiation but not after irradiation combined with burn. Oxid Med Cell Longev. 2014; 2014:481392. [PubMed: 24738019]
53. Kiang JG, Smith JT, Anderson MN, Umali MV, Ho C, Zhai M, et al. A novel therapy, using Ghrelin with pegylated G-CSF, inhibits brain hemorrhage from ionizing radiation or combined radiation injury. Pharmacy & Pharmacology International Journal. 2019; 7(3):133–45. [PubMed: 34368440]
54. Kiang JG, Garrison BR, Gorbunov NV. Radiation combined injury: DNA Damage, apoptosis, and autophagy. Adaptive Med. 2010; 2(1):1–10.
55. Kuefner MA, Brand M, Engert C, Schwab SA, Uder M. Radiation induced DNA double-strand breaks in radiology. Rofo. 2015; 187(10):872–8. [PubMed: 26333102]

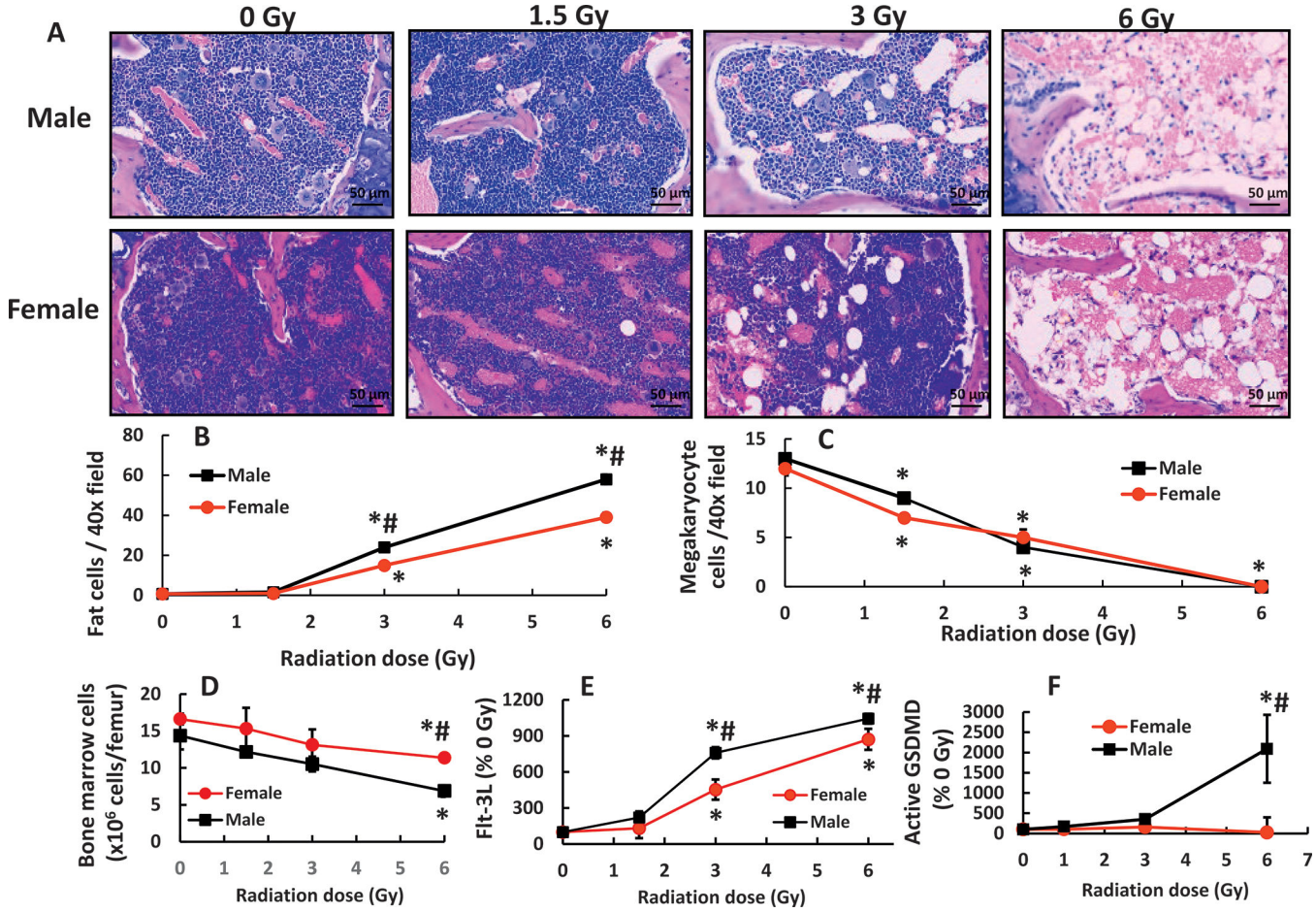

FIG. 1.

Mixed-field (67% neutron + 33% gamma) radiation injures bone marrow morphology more in male mice than in female mice. Bone marrow histology slides on day 7 post-mixed-field irradiation stained with hematoxylin and eosin (panel A). N = 4 per group. Fat cells (panel B) and megakaryocyte counts (panel C). N = 4 per group, 4 fields/slide with ×40 magnification were measured. Panel D: Bone marrow cells collected from femurs were counted. N = 4 per group. Panel E: Flt-3 ligand concentrations in blood were measured (N = 4 per group). Panel F: Active gasdermin D (GSDMD) was measured in bone marrow cell lysate from femurs (N = 3–4 per group). Data are shown as mean ± sem except Flt-3 ligand data which were mean ± sd. *P < 0.05 vs. 0 Gy; #P < 0.05 male vs. female.

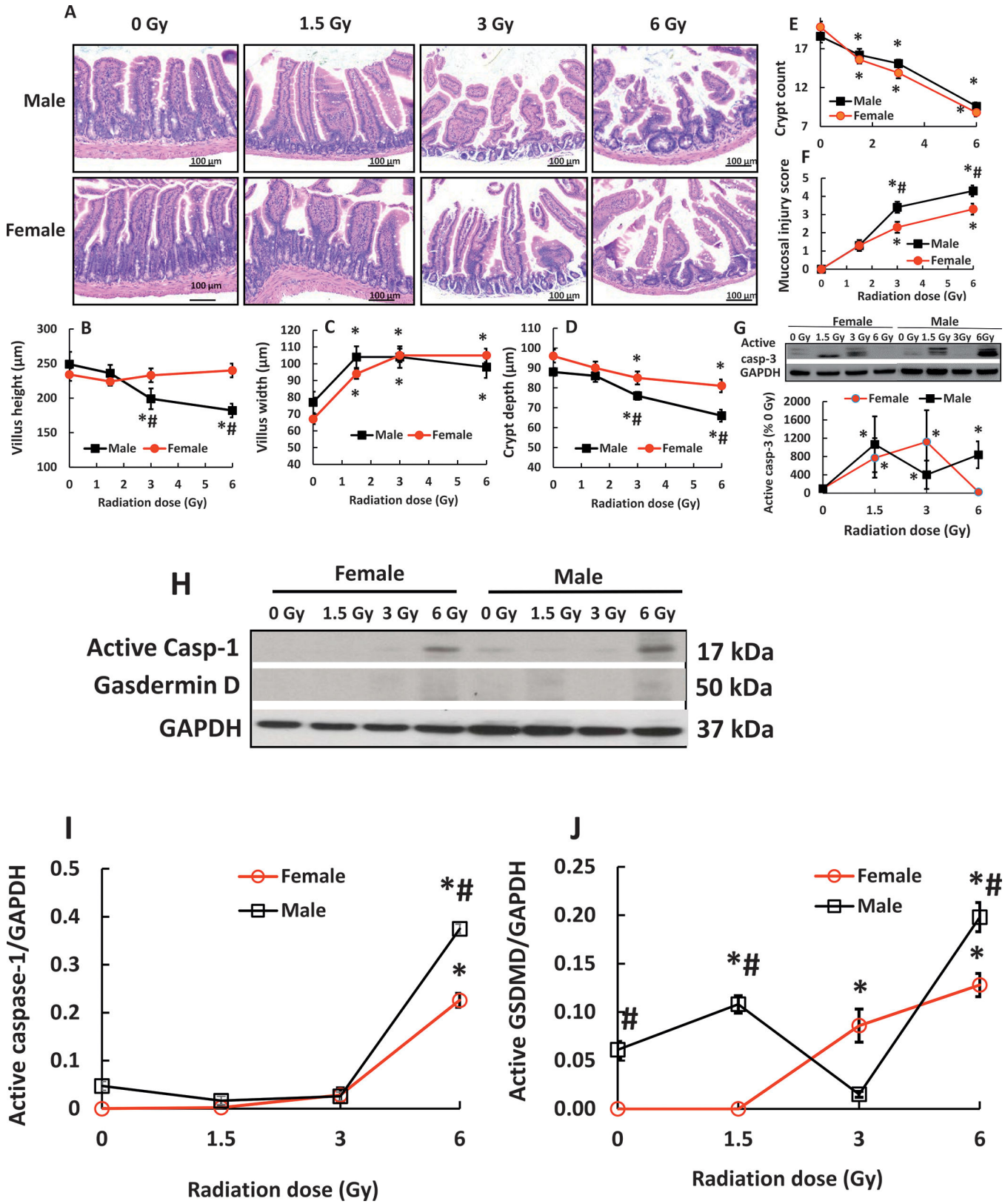

FIG. 2.

Mixed-field (67% neutron + 33% gamma) radiation injures ileum morphology more in male mice than in female mice. Panel A: Histology slides stained with hematoxylin and eosin of ileums collected on day 7 post-mixed-field irradiation. N = 4 per group. Panel B–F: Parameters of ileums including villus heights and width, crypt depth and counts, and submucosal injury scores were assessed. Panel G: Representative gels of active caspase-3 levels on day 7 were conducted using Western blotting analysis. Panel H: Representative gels of active caspase-1 levels and gasdermin D on day 7. Panel I: Active caspase-1 Panel J: Active Gasdermin D (GSDMD). The blotting intensity was quantitated densitometrically (N = 3–4 per group). Data are shown as mean ± sem. *P < 0.05 vs. 0 Gy; #P < 0.05 vs. female. Active casp-3: active caspase-3.

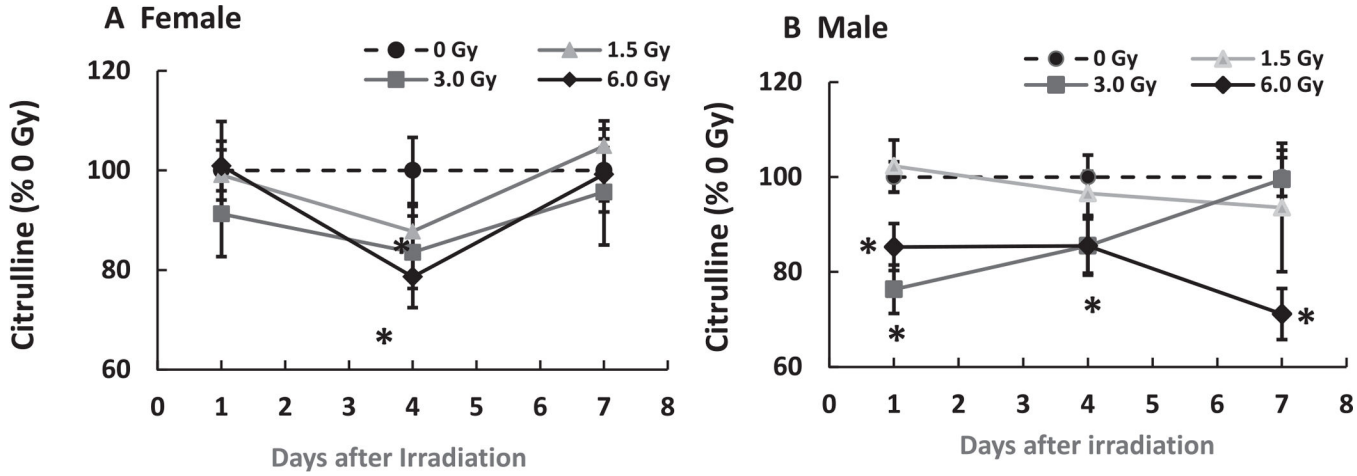

FIG. 3.

Mixed-field (67% neutron + 33% gamma) radiation alters citrulline in ileum of female mice less than male mice. N = 4 per group. Panel A: Female; Panel B: Male. Data are shown as mean ± sem. *P < 0.05 vs. 0 Gy.

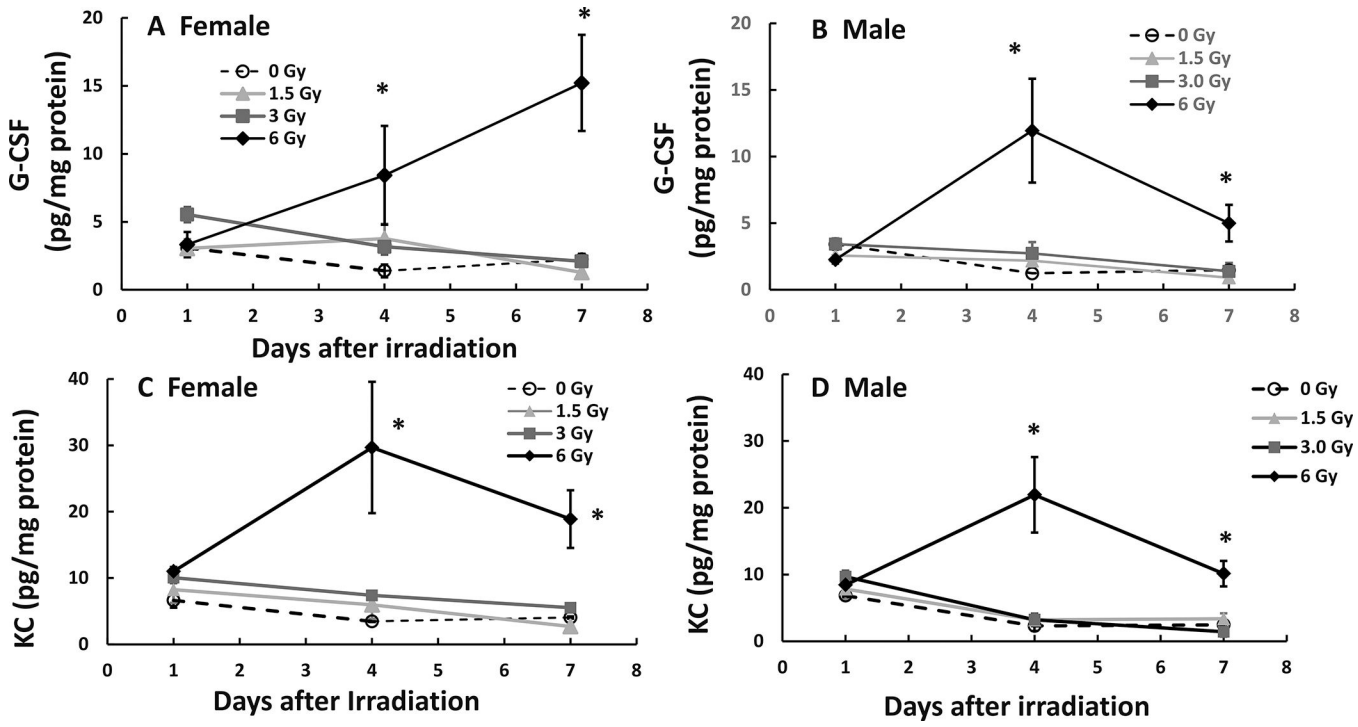

FIG. 4.

Mixed-field (67% neutron + 33% gamma) radiation sustains increases in G-CSF in ileum of female mice but not male mice. N = 4 per group per time point. G-CSF and KC in ileum samples from each mouse exposed to different mixed-field radiation doses and collected at each time point were measured by multi-plex fluid phase antibody-based analysis. Panel A: G-CSF in female mice; Panel B: G-CSF in male mice; Panel C: KC in female mice; Panel D: KC in male mice. Data are shown as mean ± sem. *P < 0.05 vs. 0 Gy at respective time point.

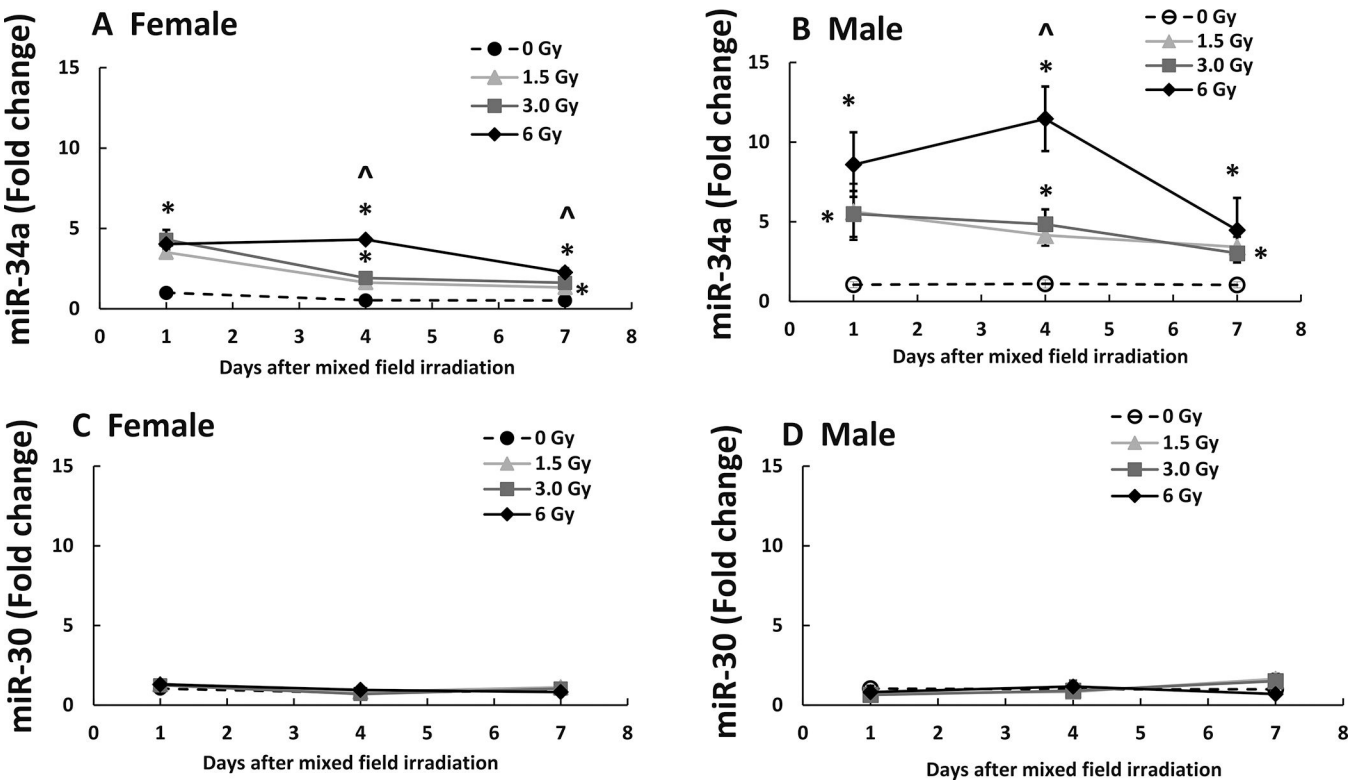

FIG. 5.

Mixed-field (67% neutron + 33% gamma) radiation increases miR-34a in ileum of female mice less than male mice. N = 4 per group per time point. MiR-34a and miR-30 in ileum samples from each mouse exposed to different mixed-field radiation doses and collected at each time point were measured by RT-PCR. Panel A: miR-34a in female mice; Panel B: miR-34a in male mice; Panel C: MiR-30 in female mice; Panel D: miR-30 in male mice. Data are shown as mean fold change ± sem. *P < 0.05 vs. 0 Gy at respective time point; ^P < 0.05 vs. 1.5 Gy and 3 Gy at respective time point.

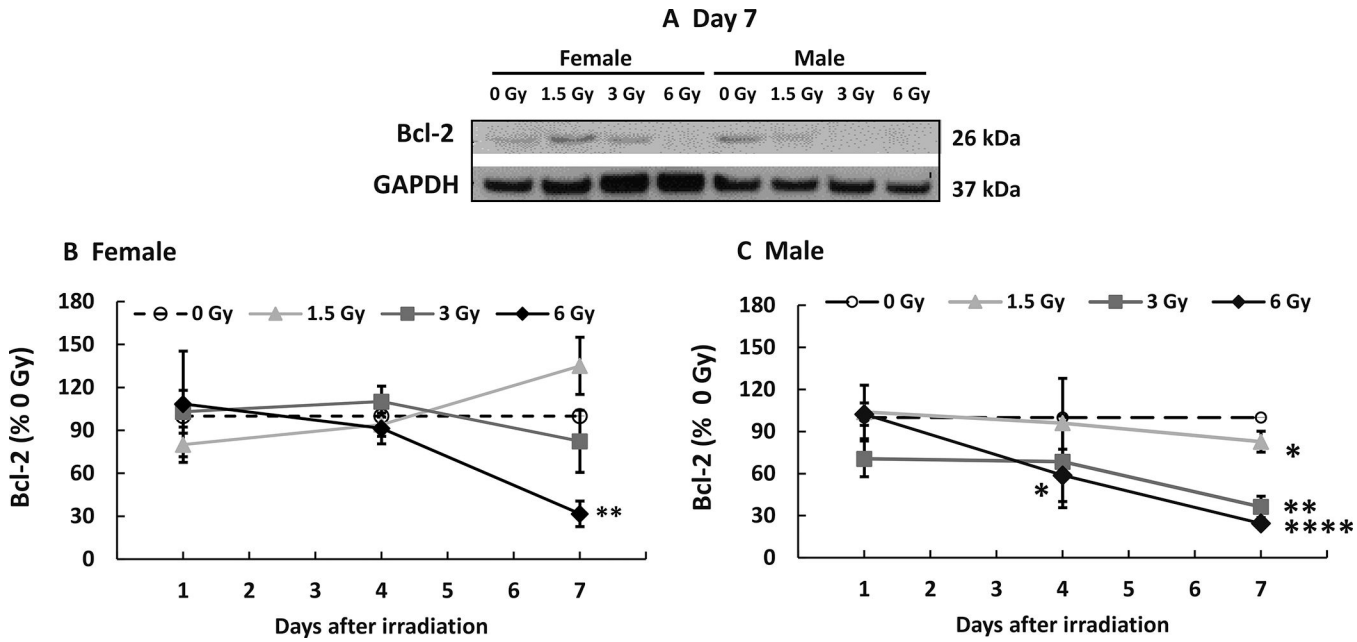

FIG. 6.

Mixed-field (67% neutron + 33% gamma) radiation decreases Bcl-2 in ileum of female mice less than male mice. N = 4 per group per time point. Bcl-2 in ileum samples from each mouse exposed to different mixed-field radiation doses and collected at each time point were measured by Western blot. Panel A: Representative gels on day 7. Densitometry graphs of (panel B) Female mice; Panel C: Male mice. Data are shown as the mean percent of 0 Gy (sham) mean values ± sem at each respective time point. *P < 0.05, **P < 0.01, ****P < 0.0001.

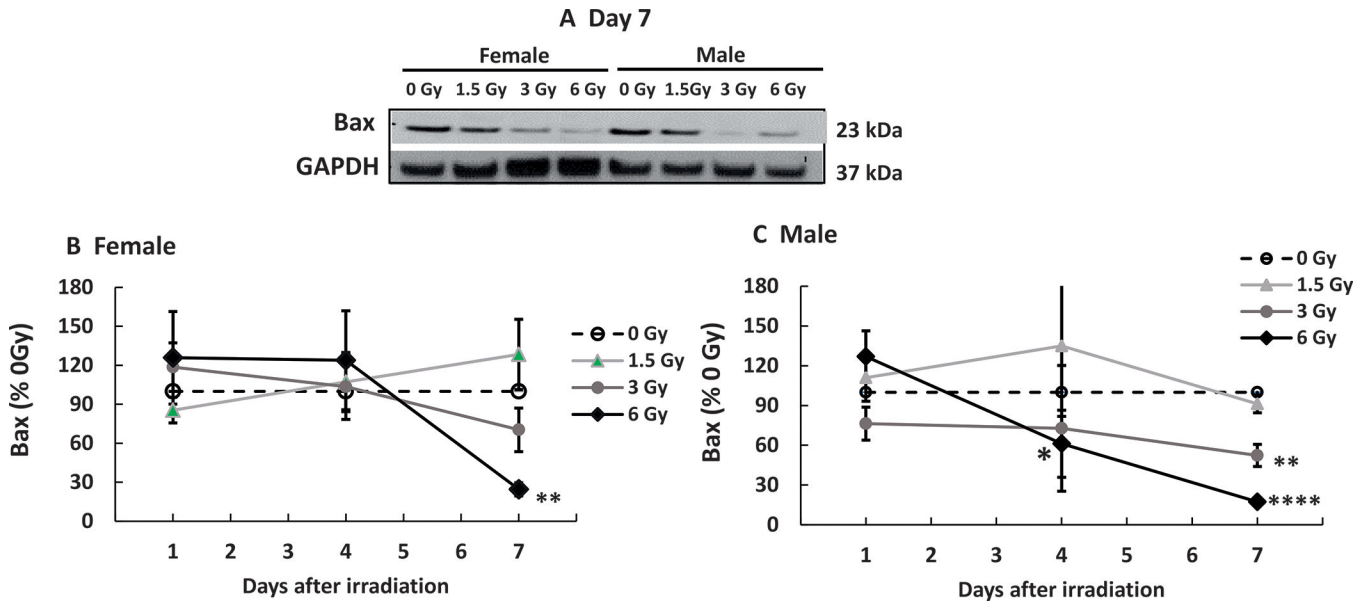

FIG. 7.

Mixed-field (67% neutron + 33% gamma) radiation alters Bax in ileum of female mice less than males. N = 4 per group per time point. Bax in ileum samples from each mouse exposed to different mixed-field radiation doses and collected at each time point were measured by Western blot. Panel A: Representative gels on day 7. Densitometry graphs of (panel B) female mice and (panel C) Male mice. Data are shown as the mean percentage of 0 Gy (sham) values ± sem at respective each respective time point. *P < 0.05, **P < 0.01, ****P < 0.0001 vs. 0 Gy.

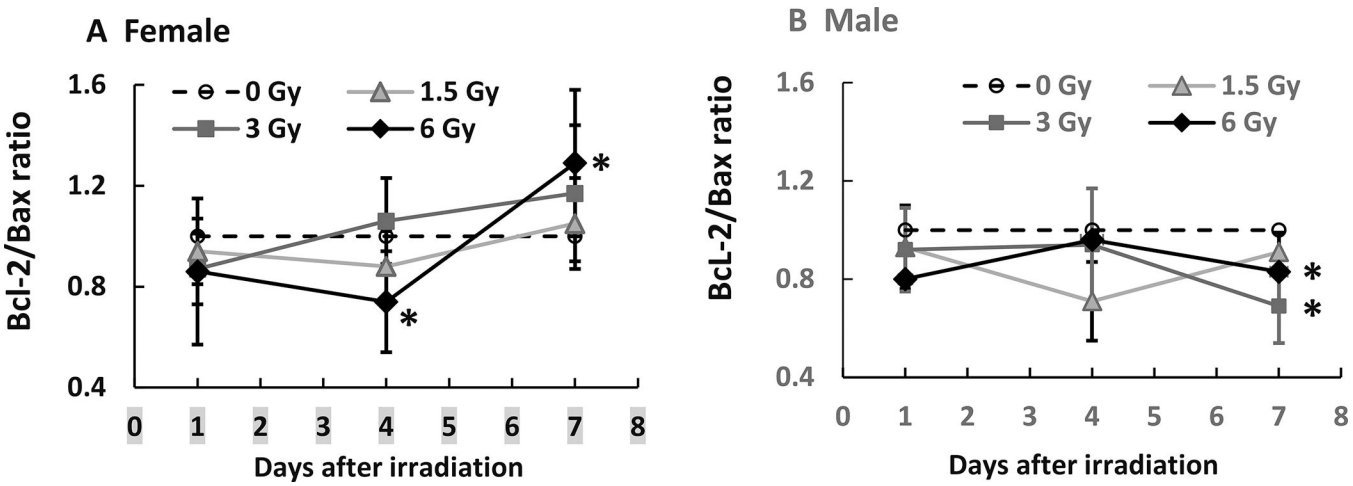

FIG. 8.

Mixed-field (67% neutron + 33% gamma) radiation increases Bcl-2/Bax ratios in ileum of female mice more than male mice. N = 4 per group per time point. Panel A: Female; Panel B: Male. *P < 0.05 vs. 0 Gy at respective time point.

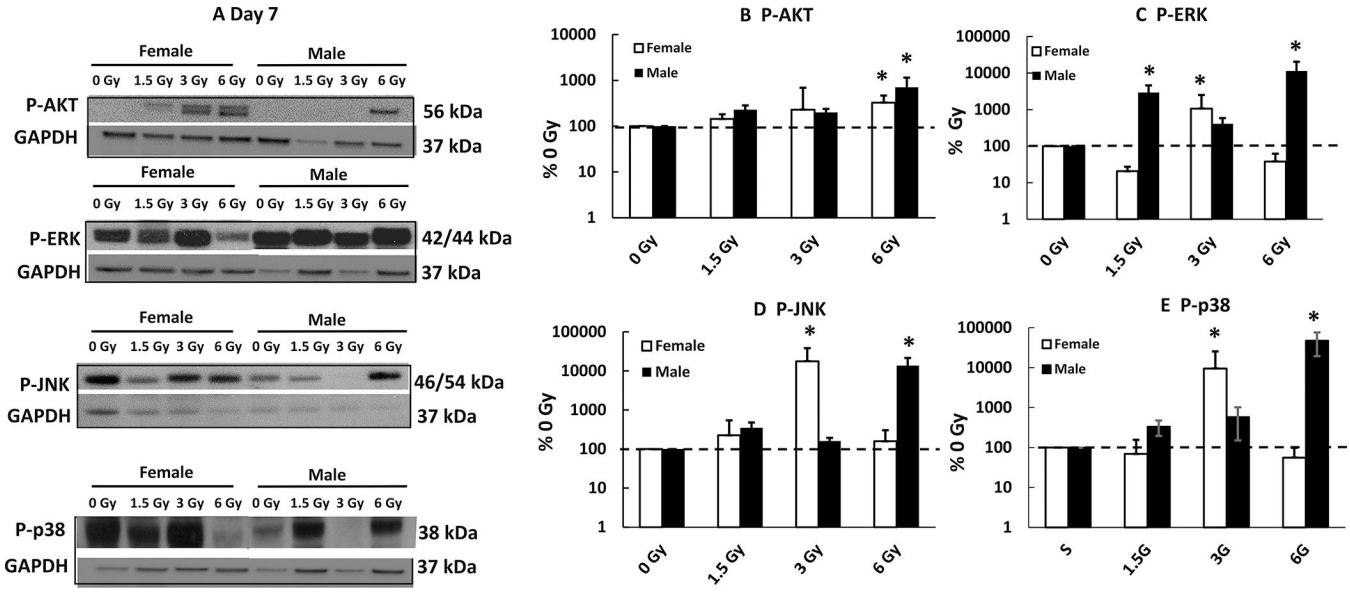

FIG. 9.

Mixed-field (67% neutron + 33% gamma) radiation alters AKT and MAPK activation in ileum of female mice less than male mice. AKT and MAPK phosphorylation in ileum samples from each mouse exposed to different mixed-field radiation doses on day 7 postirradiation was measured. Post A: Representative gels on day 7; Panel B–E: Densitometry data for each protein of interest. Data are shown as mean ± sem. *P < 0.05 vs. 0 Gy at respective time point. P-AKT: phosphorylated; P-ERK: phosphorylated ERK; P-JNK: phosphorylated JNK; P-p38: phosphorylated p38.

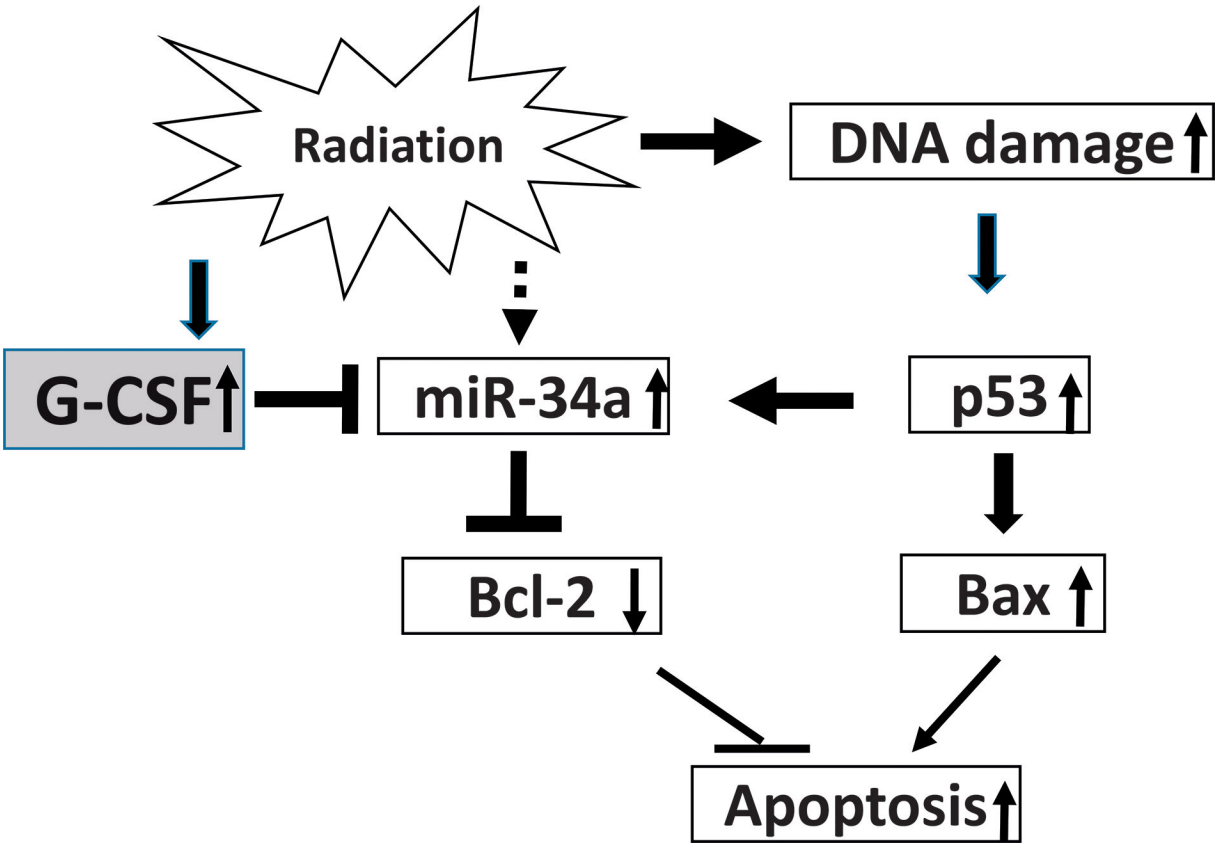

FIG. 10.

Possible mechanisms with signaling steps. Mixed-field (67% neutron + 33% gamma) radiation induces increases in miR-34a and DNA double strand breaks. The DNA damage-induces p53 activation which stimulates increases in Bax production and may be furthered miR-34a induction. Cell apoptosis may be increased due to p53-induced Bax increases and the miR-34a-inhibition of Bcl-2. The sustained increases in G-CSF in female mice may inhibit miR-34a production. Subsequently, Bcl-2 production may be increased due to the G-CSF-induced miR-34a inhibition. Therefore, apoptotic death may be dropped down in the female ileum.

TABLE 1

The Study Design with Female Mice and Male Mice, Respectively

	0 Gy (sham)	1.5 Gy	3 Gy	6 Gy
Day 1	N = 4	N = 4	N = 4	N = 4
Day 4	N = 4	N = 4	N = 4	N = 4
Day 7	N = 4	N = 4	N = 4	N = 4